IEEE Access
Multidisciplinary ⋮ Rapid Review ⋮ Open Access Journal

Received July 15, 2020, accepted August 10, 2020, date of publication August 19, 2020, date of current version August 31, 2020.

Digital Object Identifier 10.1109/ACCESS.2020.3017746

Anti-Injury Function of Complex Spiking Neural Networks Under Random Attack and Its Mechanism Analysis

LEI GUO[1,2], RUIXUE MAN[1,2], YOUXI WU[3], (Member, IEEE), HUAN LV[1,2], AND HONGLI YU[1,2]

[1]State Key Laboratory of Reliable and Intelligence of Electrical Equipment, Hebei University of Technology, Tianjin 300130, China
[2]Tianjin Key Laboratory of Bioelectromagnetic Technology and Intelligent Health, Hebei University of Technology, Tianjin 300130, China
[3]School of Artificial Intelligence, Hebei University of Technology, Tianjin 300401, China

Corresponding author: Lei Guo (guolei@hebut.edu.cn)

This work was supported in part by the Natural Science Foundation of Hebei Province under Grant E2020202033; and in part by the National Natural Science Foundation of China under Grant 615711880, Grant 61976240, and Grant 51877068.

ABSTRACT The biological brain has self-adaptive ability through neural information processing and regulation. Drawing from the advantage of the biological brain, it is significant to research the robustness of artificial neural network (ANN) based on brain-like intelligence. In this study, based on the Izhikevich neuron model and the synaptic plasticity model which contains excitatory and inhibitory synapses, a spiking neural network (SNN) with small-world topology and a SNN with scale-free topology are constructed. The anti-injury function of two complex SNNs (CSNN) under random attack is comparatively analyzed. On this basis, the information processing of CSNN under attack is further discussed, and the anti-injury mechanism of CSNN is explored based on the synaptic plasticity. The experimental results show that: (1) scale-free SNN (SFSNN) has better performance than small-world SNN (SWSNN) in the anti-injury ability under random attacks. (2) The information processing of CSNN under random attacks is clarified by the linkage effects of dynamic changes in neuron firing, synaptic weight, and topological characteristics. (3) The anti-injury ability of CSNNs is closely related to the dynamic evolution of synaptic weight, which implies the dynamic regulation of synaptic plasticity is the intrinsic factor of the anti-injury function of CSNNs. This study lays a theoretical foundation for the application of brain-like intelligence with adaptive fault-tolerance.

INDEX TERMS Complex network, spiking neural network, random attack, anti-injury function, anti-injury mechanism.

I. INTRODUCTION

With the emergence of the latest achievements in brain science, a new round of artificial intelligence research upsurge has been triggered. The biological brain has self-adaptive ability through neural information processing and regulation [1]. Drawing from the advantage of the biological brain, it is significant to research the robustness of artificial neural network (ANN) based on brain-like intelligence. Spiking neural network (SNN) is the most biologically interpreted ANN and has been applied in many fields, such as speech recognition [2], geological monitoring [3], and tumor detection [4]. There are three elements of constructing a SNN: neuron model, synaptic plasticity model, and network topology. Extensive biological researches have proved that brain networks have the scale-free properties and/or the small-world properties [5], [6]. Bin *et al.* [7] used electroencephalogram (EEG) to establish brain functional networks, which found that the network has high clustering coefficient characteristics of small-world networks, and the degree distribution is in line with the power-law distribution property of scale-free networks. The structure of the network has a profound influence on the dynamic process of the network. Therefore, drawn from the research results of biological brain network, many researches have been carried out based on the SNN with complex network topology. Kim and Lim [8] employed the scale-free network with connection probability of 0.1 to construct a SNN, and investigated the effects

The associate editor coordinating the review of this manuscript and approving it for publication was Haruna Chiroma.

of network architecture on stochastic burst synchronization. Boaretto *et al.* [9] studied a SNN with 2000 neurons connected in a small-world network topology with nonlocal connection probability of 0.001, and proposed a method that can control the anomalous synchronization and non-stationarity occurring without any effect on the individual neuron dynamics. The Hebbian hypothesis suggests that the synaptic plasticity is the nerve basis of learning and memory through information transmission. Reference [10] proposed an adaptive scale-free neural network regulated by excitatory synaptic plasticity, which found that spike-timing-dependent plasticity can optimize coherence resonance and synchronization transitions by autaptic delay. However, inhibitory synapses also play an important regulative role in the biological brain [11]. It is necessary to introduce a synaptic plasticity model which including excitatory and inhibitory synapses in the SNN to investigate the brain information processing. Lin *et al.* [12] constructed a SNN regulated by excitatory and inhibitory synapses coexisted, which found that inhibitory neurons can inhibit synchronization by delaying the firing of the neurons and promote synchronization by facilitating the transition of the oscillatory patterns. Combining with the latest progress of network topology and synaptic plasticity in the biological brain, the exploration of the SNN with more biological rationality can promote the development of brain-like intelligence.

Brain-like research is to simulate the structure and function of the real brain as much as possible based on the latest findings in brain science. Extensive biological experiments in neuroscience indicate that the brain network has a strong fault-tolerant ability. Based on the size of the largest network component and global efficiency, Alstott *et al.* [13] analyzed the change of functional connection under ''random'' and ''targeted'' node deletions on the structural brain network model based on diffusion spectrum imaging (DSI). It found that the brain network is relatively resilient against random node removal and target node removal. Joyce *et al.* [14] conducted network attack experiments on voxel-wise functional brain networks and region-of-interest (ROI) networks generated based on functional magnetic resonance imaging (fMRI). Based on local and global efficiency as well as the size of the giant component, the impact of targeted attacks on network structure was evaluated. It found that the structure of the brain network is highly resilient to targeted attacks. A growing number of studies approach the brain as a complex network [15]. Many studies have analyzed the robustness of complex networks under attack. For example, Albert and Jeong [16] found that the scale-free network has high robustness to random attacks and is very vulnerable at target attacking some important nodes, by analyzing the index of average shortest path length. He *et al.* [17] studied the robustness of small-world networks and scale-free networks under different attacks based on the index of total connectedness, which found that the scale-free network is more robust under random attacks; the small-world network is more robust under target attacks. Although past studies have shown that small-world networks and scale-free networks have certain anti-injury abilities, these findings are from the static network without nerve electrophysiological characteristics. In other words, for the networks in these studies, a node is just a point, not a neuron model, and an edge is just a line, not a synapse model. As is known to all, the biological brain has the self-adaptive dynamic regulation ability to external attacks through information processing. The SNN with neuronal dynamics and synaptic plasticity is the dynamic network with self-adaptive regulation ability. Therefore, the exploration of the anti-injury function of the SNN with nerve electrophysiological characteristics is meaningful, and it can promote the development of brain-like intelligence with fault-tolerance. In this study, the relative change rate of firing rate and the correlation between membrane potential of neurons are used as indexes to investigate the anti-injury function of two kinds of SNN with complex network topology under random attacks. Then, the information processing of the network is further analyzed, and the anti-injury mechanism of the network is explored.

The main contributions of this study are as follows:

- The two kinds of complex SNN (CSNN) which have more biological rationality are constructed: small-world SNN (SWSNN) and scale-free SNN (SFSNN), which promotes the development of SNN in brain-like intelligence.
- The robustness of the CSNNs with nerve electrophysiological characteristics under random attack is comparatively analyzed. The experimental results show that SFSNN has better performance than SWSNN in the anti-injury ability, which lays a theoretical foundation for engineering applications with fault-tolerant ability by drawing from the advantage of the biological brain.
- The information processing of CSNN under random attacks is clarified by the linkage effects of dynamic changes in neuron firing, synaptic weight, and topological characteristics. The findings are helpful to understand brain information processing.
- The relationship between the external anti-injury ability of CSNN and the internal synaptic plasticity is established. The experiment results show the dynamic regulation of synaptic plasticity is significantly related to the anti-injury ability of CSNN, which implies that the dynamic regulation of synaptic plasticity is the intrinsic factor of the anti-injury function of CSNNs.

The rest of this study is organized as follows: In Section II, the two kinds of CSNNs are constructed. In Section III, the anti-injury ability of two kinds of networks is investigated under random attack. In Section IV, the anti-injury mechanism of CSNN is further analyzed. We present the conclusion in Section V.

II. CONSTRUCTION OF CSNN

In this study, we construct two kinds of CSNNs: a SNN with small-world network topology and a SNN with scale-free network topology. The Izhikevich neuron model is used as the node of CSNNs, and the synaptic plasticity model with excitatory and inhibitory synapses coexisted is used as the edge of CSNNs.

A. IZHIKEVICH NEURON MODEL

At present, there are many spiking neuron models. Among these, the Hodgkin-Huxley (HH) model is the most biologically interpretable spiking neuron model. Since the model consists of fourth-order partial differential equations, its time complexity is high. The first-order Leaky Integrate-and-Fire (LIF) model is the simplest spiking neuron model, which has low time complexity but poor biological interpretation. The second-order Izhikevich neuron model combines the advantages of the HH model and LIF model, which can not only well reflect the firing characteristics of biological neurons but also be suitable for large-scale simulation computing due to its low time complexity [18]. Therefore, we choose the Izhikevich neuron model as the node of CSNNs. The model is defined as:

$$\begin{aligned} \frac{\mathrm{d}v}{\mathrm{d}t} &= 0.04v^2 + 5v + 140 - u + I, \\ \frac{\mathrm{d}u}{\mathrm{d}t} &= a(bv - u), \quad \text{if } v \geq 30, \begin{cases} v \leftarrow c \\ u \leftarrow u + d, \end{cases} \end{aligned} \tag{1}$$

where v is the membrane potential; u is the membrane voltage recovery variable, which reflects the activation of potassium channel current and the inactivation of sodium channel current in biological neurons and provides negative feedback for the membrane voltage; I is the sum of the external input current and the synaptic current transmitted through multiple synapses. a, b, c, and d are dimensionless parameters. Different parameter values correspond to different types of neurons in the model. In this study, excitatory neurons and inhibitory neurons are randomly distributed in a ratio of 4:1 in CSNNs according to the experimental results of neuroanatomy [19]. The regular spiking (RS) pattern is used as the firing pattern of excitatory neurons in the CSNNs, whose parameters $a = 0.02$, $b = 0.2$, $c = -65$, and $d = 8$, as shown in Fig. 1(a). The low-threshold spiking (LTS) pattern is used as the firing pattern of inhibitory neurons, whose parameters $a = 0.02$, $b = 0.25$, $c = -65$, and $d = 2$, as shown in Fig. 1(b).

B. SYNAPTIC PLASTICITY MODEL

The synaptic plasticity model with excitatory synapses and inhibitory synapses coexisted is used to construct CSNNs. The output current and input voltage of the synaptic plasticity model show an approximately linear relationship, which can be described as:

$$I_{syn} = g_{syn}(t)(V - V_m(t)), \tag{2}$$

where I_{syn} is the synaptic currents; g_{syn} is the synaptic conductance; $V_m(t)$ is the membrane potential of a postsynaptic neuron; V is the inversion of potential. In this study, excitatory inversion potential $V^E = 0mV$; inhibitory inversion potential $V^I = -70mV$. Both excitatory and inhibitory synapses regulate the efficiency of information transmission among neurons by changing the value of synaptic conductance. Their regulation rules are as follows:

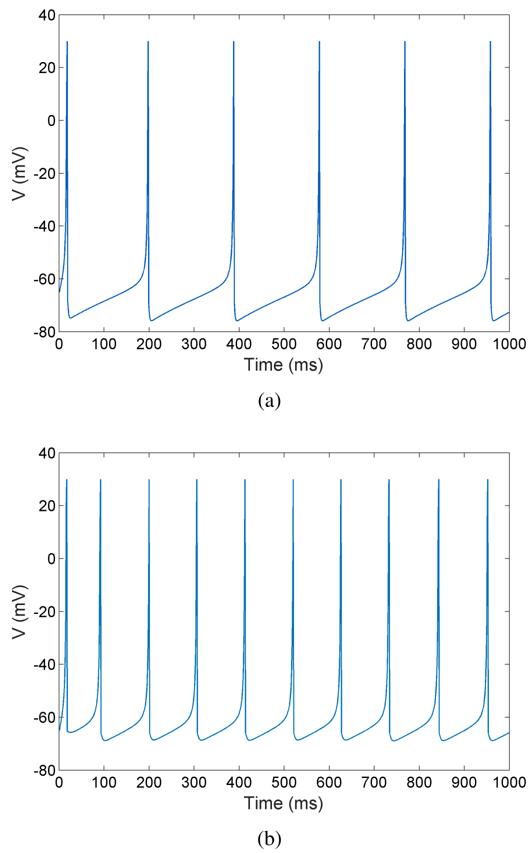

FIGURE 1. **The firing patterns of Izhikevich neurons. (a) The firing pattern of excitatory neurons. (b) The firing pattern of inhibitory neurons.**

(1) If postsynaptic neuron j has not received the action potential of presynaptic neuron i, the synaptic weights of excitatory and inhibitory synapses decline exponentially, which are described by equations (3) and (4), respectively.

$$\text{Excitatory synapse: } \tau_{ex}\frac{\mathrm{d}g_{ex}}{\mathrm{d}t} = -g_{ex}, \tag{3}$$

$$\text{Inhibitory synapse: } \tau_{in}\frac{\mathrm{d}g_{in}}{\mathrm{d}t} = -g_{in}, \tag{4}$$

where τ_{ex} and τ_{in} represent the decay constants of excitatory and inhibitory synaptic conductance, respectively. In this study, $\tau_{ex} = \tau_{in} = 5ms$.

(2) If postsynaptic neuron j has received the action potential of presynaptic neuron i, the weight $g_{ex}(t)$ of excitatory synapse and $g_{in}(t)$ of inhibitory synapse are as follows:

$$\text{Excitatory synapse: } g_{ex}(t) \rightarrow g_{ex}(t) + \bar{g}_{ex}, \tag{5}$$

$$\text{Inhibitory synapse: } g_{in}(t) \rightarrow g_{in}(t) + \bar{g}_{in}, \tag{6}$$

where $\bar{g}_{ex}$ and $\bar{g}_{in}$ represent the excitatory and inhibitory synaptic conductance increment caused by action potential, respectively. $\bar{g}_{ex}$ is regulated by the synaptic correction function w_{ij}, $\bar{g}_{in}$ is regulated by the synaptic correction function m_{ij}.

The synaptic correction function w_{ij} and m_{ij} are as follows:

$$w_{ij} = \begin{cases} A_+ \exp(\Delta t/\tau_+) \\ -A_- \exp(\Delta t/\tau_-), \end{cases} \tag{7}$$

$$m_{ij} = \begin{cases} B_+ \exp(\Delta t/\tau_+) \\ -B_- \exp(\Delta t/\tau_-), \end{cases} \tag{8}$$

where Δt is the firing interval between presynaptic neuron and postsynaptic neuron; τ_+ and τ_- represent the time interval between the firing of neurons before and after synaptic strengthening and synaptic weakening, respectively; A_+ and A_- represent the maximum and minimum modified values of the synaptic conductance of excitatory synapses when they are strengthened and weakened, respectively; B_+ represent the maximum and minimum corrections of the synaptic conductance of the inhibitory synapse when it increases and decreases, respectively. According to empirical studies [20], the parameters are: $\tau_+ = \tau_- = 20ms$, $A_+ = 0.1$, $A_- = 0.105$, $B_+ = 0.02$, and $B_- = 0.03$ in this study.

C. COMPLEX NETWORK TOPOLOGY MODEL

We generate two kinds of complex networks based on the generation algorithm. One is the small-world network with high small-world property, and the other is the scale-free network whose degree distribution follows power-law distribution. Through our experiments, the size of both networks is set as 500 nodes for the following reasons: when the number of network nodes is more than 1000, the running of the program need use a computer cluster for calculation, rather than a single computer due to the time complexity of the calculation; we find that the anti-injury performance of CSNNs with the number of nodes in the range of 500-1500 shows no obvious difference according to the results of our experiments. The network construction and analysis are implemented on a PC with a 2.50 GHz CPU and 8 GB RAM.

1) SMALL-WORLD NETWORK

The small-world network topology of the SWSNN in this study is generated by the WS algorithm [21]. In the WS algorithm, the small-world topologies with different clustering coefficients can be obtained by adjusting the rewiring probability p_c. Small-world property σ of the network can be quantitatively analyzed, and its description is as follows:

$$\sigma = \frac{\gamma}{\lambda} = \frac{C_{real}/C_{random}}{L_{real}/L_{random}}, \tag{9}$$

where C_{real} and C_{random} represent the average clustering coefficient of the real network and its corresponding random network respectively, L_{real} and L_{random} represent the average shortest path length of the real network and its corresponding random network respectively, γ is the ratio between C_{real} and C_{random}, and λ is the ratio between L_{real} and L_{random}. That is, the small-world property of the network is relative to the random network corresponding to this network. Through

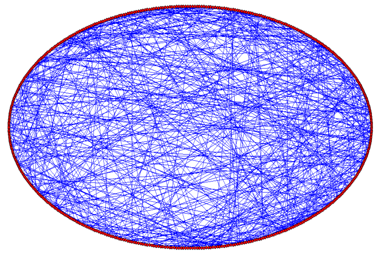

(a)

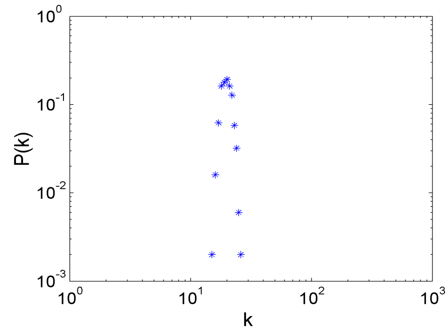

(b)

FIGURE 2. The topology and degree distribution of small-world network. (a) Topological diagram. The red nodes on ellipse boundary represents the nodes of network, the internal blue line represents the connections between nodes. (b) Degree distribution. The abscissa represents the node degree value, the ordinate represents the frequency of the corresponding degree value in the network. The degree distribution of nodes in small-world network is concentrated.

experiments, we find that the small-world network with $p_c = 0.2$ has the highest σ, which is 9.1209. Therefore, the topology of SWSNN is the small-world network with $p_c = 0.2$, and its topology and degree distribution are shown in Fig. 2(a) and (b), respectively. And the characteristic parameters of the network are shown in Table 1.

2) SCALE-FREE NETWORK

The scale-free network topology of the SFSNN in this study is generated by the BBV algorithm [22]. In the BBV algorithm, the scale-free topologies with different clustering coefficients can be obtained by adjusting the dot probability p_p. The degree distribution of scale-free networks follows power-law distribution and its power-law index η is between 2 and 3. The η can reflect the scale-free property of a network. Extensive biological experiments have proved that the brain functional network has a high clustering coefficient, and whose η of the scale-free property is about 2 [23]. Through experiments, we find that when $p_p = 0.3$, the η of the scale-free network is 2.154, and the clustering coefficient is more than 0.5, satisfying the characteristics of the brain functional network. Therefore, the scale-free network with $p_p = 0.3$ is used as the topology of SFSNN, whose topology and degree distribution are shown in Fig. 3(a) and (b), respectively. And the characteristic parameters of the network are shown in Table 2.

From the above, the degree distribution of the scale-free networks in our study follows the power-law distribution,

TABLE 1. The characteristic parameters of small-world network.

p_c (%)	Average degree	Average clustering coefficient	Average shortest path length	γ	λ	σ
0.2	20.0000	0.3801	2.6554	10.1090	1.1080	9.1209

TABLE 2. The characteristic parameters of scale-free network.

p_p (%)	Average degree	Average clustering coefficient	Average shortest path length	γ	λ	σ	η
0.3	9.9760	0.5237	2.4407	1.2545	0.9916	1.2651	2.1540

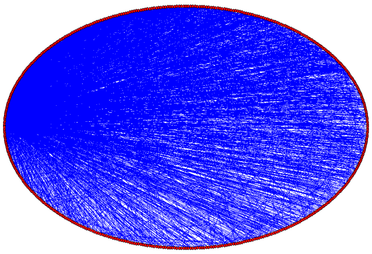

(a)

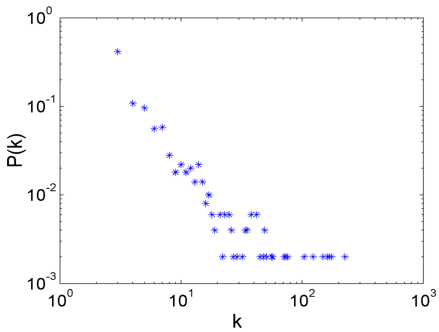

(b)

FIGURE 3. The topology and degree distribution of scale-free network. (a) Topological diagram. The red nodes on ellipse boundary represents 500 nodes, the internal blue line represents the connections between nodes. (b) Degree distribution. The abscissa represents the node degree value, the ordinate represents the frequency of the corresponding degree value in the network. The degree distribution of scale-free network follows the power-law distribution.

whereas that of the small-world network in our study does not. That is, the small-world network does not have scale-free properties. And the small-world property of the scale-free network is far lower than that of the small-world network. That is, this scale-free network mainly presents scale-free properties. Additionally, there are obvious differences between the two complex networks in average degree, average clustering coefficient, average shortest path length, γ, λ. Therefore, the two complex networks can represent the small-world network topology structure and the scale-free network topology structure, respectively. In this study, a SFSNN and a SWSNN are constructed by employing the Izhikevich neuron model and the synaptic plasticity. The SNNs based on the two complex network topology structures can present different brain-like functions.

III. ANTI-INJURY FUNCTION OF CSNN UNDER RANDOM ATTACK

To investigate the anti-injury function of two kinds of CSNNs under random attacks, the anti-injury abilities of two kinds of CSNNs are evaluated based on the two indexes of the relative change rate of firing rate and the correlation between membrane potential. We randomly remove neurons in CSNNs to represent the neuron injury caused by the attack. The proportion P of injured neurons in CSNNs ranges from 5% to 50%, and the step length is 5%.

A. THE RELATIVE CHANGE RATE OF FIRING RATE

1) FUNDAMENTAL PRINCIPLE

The firing rate is the number of spikes emitted by neurons per unit time. In this study, the firing rate of CSNN is the average of all neurons in the network. To quantitatively analyze the change in firing rate before and after the attack, the relative change rate of firing rate is introduced, which is described as follows:

$$\delta\% = \frac{|f_j - f_i|}{f_i} * 100\%, \tag{10}$$

where f_i and f_j represent the firing rate of the network before and after the attack respectively, and δ represents the relative change rate of the firing rate before and after the attack. The smaller the δ is, the stronger the anti-injury ability of CSNN is.

2) EXPERIMENTAL RESULTS AND ANALYSIS

To investigate the anti-injury abilities of SFSNN and SWSNN under random attacks, the change in the firing rate of neurons in the two networks before and after the attack is comparatively analyzed. The relative change rate of the firing rate δ of the two kinds of CSNNs under different P is shown in Fig. 4.

From Fig. 4, with the increase of P, the δ of SWSNN increases rapidly, and its distribution is between 0.40% and 8.94%, whereas the δ of SFSNN grows slowly, and its distribution is between 0.64% and 4.11%. Except for the $P = 10\%$, the δ of SFSNN is lower than that of SWSNN. The results indicate that both CSNNs have a certain anti-injury function,

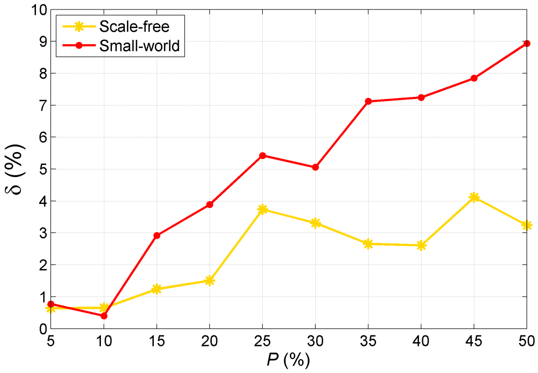

FIGURE 4. **The relative change rate of the firing rate of SFSNN and SWSNN under different *P*.**

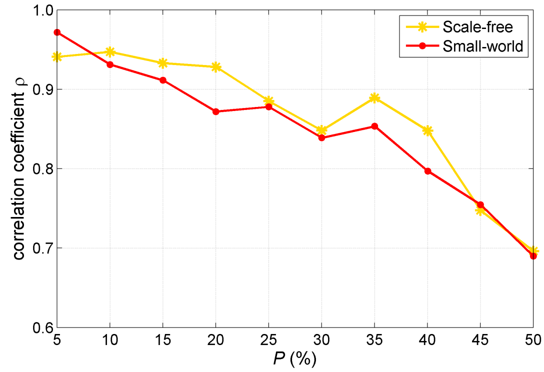

FIGURE 5. **The correlation coefficient of SFSNN and SWSNN under different *P*.**

and the anti-injury ability of SFSNN is stronger than SWSNN under random attacks.

B. THE CORRELATION BETWEEN MEMBRANE POTENTIAL

1) FUNDAMENTAL PRINCIPLE

The correlation between membrane potential of a neuron can reflect the similarity of neuronal membrane potential before and after the attack. The correlation between membrane potential of CSNN is the average correlation between membrane potential of all neurons in the network. The correlation coefficient can be described as follows:

$$\rho_{ij}(\tau) = \frac{\sum_{t=t_1}^{t_2-\tau+1} x_i(t)x_j(t+\tau)}{\sqrt{\sum_{t=t_1}^{t_2-\tau+1} x_i^2(t) \sum_{t=t_1}^{t_2-\tau+1} x_j^2(t+\tau)}}, \tag{11}$$

where $\rho_{ij}(\tau)$ is correlation coefficient; $[t_1, t_2]$ is simulation duration; x_i is the membrane potential of neurons before attack; x_j is the membrane potential after attacks. The maximum correlation coefficient ρ in $\rho_{ij}(\tau)$ is used to evaluate the correlation between membrane potential before and after the attack. The larger the ρ is, the stronger the anti-injury ability of CSNN is.

2) EXPERIMENTAL RESULTS AND ANALYSIS

To investigate the anti-injury abilities of SFSNN and SWSNN under random attacks, the correlation between membrane potential of neurons in the two networks before and after the attack is comparatively analyzed. The correlation coefficient ρ of the two kinds of CSNNs with different P is shown in Fig. 5.

From Fig. 5, the change in the ρ of two CSNNs shows a downward trend with the increase of P, and the ρ is always larger than 0.8 at below the 35%. Except for the and $P = 5\%$ and $P = 45\%$, the ρ of SFSNN is higher than that of SWSNN. The results indicate that both CSNNs have a certain anti-injury function, and the anti-injury ability of SFSNN is stronger than SWSNN under random attacks.

Through the analysis of two indexes of the relative change rate of firing rate and the correlation between membrane potential, we find that both CSNNs have a certain anti-injury function, and SFSNN has better performance than SWSNN in the anti-injury ability under random attack. The SNN with nerve electrophysiological characteristics is the latest generation ANN. The significance of this study based on SNN is that the development of SNN in brain-like intelligence can be promoted, and the theoretical foundation for the application of SNN in clinic and engineering can be laid. And the robustness mechanism of the brain-like network can be further explored based on the neural information processing of CSNN.

IV. ANTI-INJURY MECHANISM ANALYSIS OF CSNN UNDER RANDOM ATTACK

To explore the anti-injury mechanism of CSNNs under random attacks, the information processing of the SFSNN is analyzed, and the relationship between synaptic plasticity and the anti-injury function of CSNNs is further discussed.

A. INFORMATION PROCESSING OF SFSNN

To explore the information processing of network under random attack, taking the $P = 15\%$ as an example, the dynamic evolution of neural information processing is clarified from the firing rate, synaptic weight and the shortest path length of SFSNN.

1) FIRING RATE

The firing sequence of each neuron in SFSNN changes under random attacks. This change leads to changes in the firing rate of neurons. The average firing rate of SFSNN is used to characterize the firing of all neurons. The dynamic evolution of the average firing rate of neurons with time is shown in Fig. 6.

From Fig. 6, in the first 150 ms, the average firing rate of SFSNN drops sharply; during 150-700 ms, the average firing rate drops slowly; after 700 ms, the average firing rate tends to be stable.

2) SYNAPTIC WEIGHT

Formulas (3), (4), (5), and (6) indicate that synaptic weight is determined by the firing sequence of presynaptic and

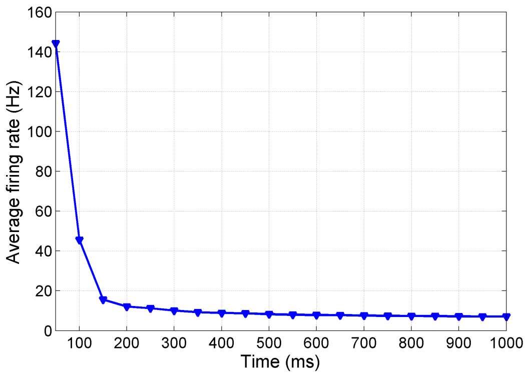

FIGURE 6. The dynamic evolution of the average firing rate of SFSNN.

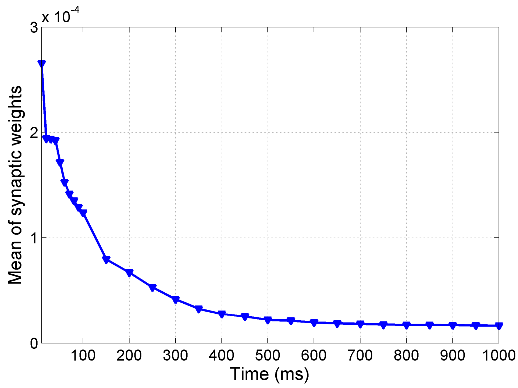

FIGURE 7. The dynamic evolution of the mean of synaptic weight of SFSNN.

postsynaptic neurons. Therefore, the firing change in neurons leads to the change in synaptic weight under random attacks. The mean of synaptic weight is used to characterize the synaptic weight of all edges in SFSNN. The dynamic evolution of the mean of synaptic weight in SFSNN under attacks is shown in Fig. 7.

From Fig. 7, in the first 150 ms, the mean of synaptic weight drops rapidly; during 150-700 ms, the mean of synaptic weight decreases slowly; after 700 ms, the mean of synaptic weight tends to be stable.

3) WEIGHTED SHORTEST PATH LENGTH

As an important index to measure the topological characteristics of complex network, the shortest path length reflects the transmission efficiency between two nodes in the network. The shortest path length d_{ij} in a weighted network is described as follows [24]:

$$d_{ij} = \min_{\Upsilon(i,j)\in\Gamma(i,j)} \left[\sum_{m,n\in\Upsilon(i,j)} \frac{1}{w_{mn}} \right], \tag{12}$$

where w_{mn} is the synaptic weight. It can be seen that the change in synaptic weight leads to the change in d_{ij}. In this study, the average shortest path length is used to characterize the shortest path length of all neuron pairs in SFSNN, and its dynamic evolution is shown in Fig. 8.

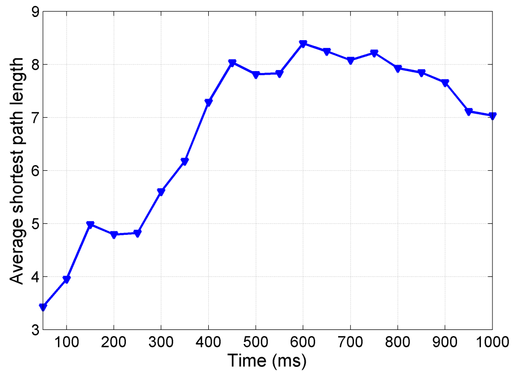

FIGURE 8. The dynamic evolution of the average shortest path length of SFSNN.

From Fig. 8, in the first 450 ms, the average shortest path length of SFSNN increases rapidly; during 500-1000 ms, the average shortest path length fluctuates little and tends to stabilize.

From the above results, the dynamic evolution of neural information processing presents a trend from violent, to moderate, to gradually stable. Under random attacks, the firing sequence of neurons in CSNN changes, which leads to the change in synaptic weight. The change in synaptic weight leads to the change in topological characteristics, which forms the self-adaptive regulation of CSNN.

B. RELATIONSHIP BETWEEN SYNAPTIC PLASTICITY AND THE ANTI-INJURY FUNCTION

To explore the relationship between synaptic plasticity and the anti-injury function of CSNNs, the dynamic regulation process of synaptic plasticity in SFSNN and SWSNN is comparatively analyzed, and the correlation between the dynamic regulation of synaptic plasticity and the anti-injury abilities of CSNNs is further investigated.

1) COMPARATIVE ANALYSIS OF REGULATION PROCESS OF SYNAPTIC PLASTICITY

To investigate the regulation process of synaptic plasticity of CSNNs under random attacks, the mean of synaptic weights of SFSNN and SWSNN with the proportion P of injured neurons of 0%, 5%, 15%, 25%, 35%, and 45% are analyzed. The dynamic evolution of the mean of synaptic weight under different P is shown in Fig. 9.

From Fig. 9(a), the dynamic evolution processes of the mean of synaptic weight of the SFSNN injured randomly is not obviously different from that of the uninjured. From Fig. 9(b), the dynamic evolution process of the mean of synaptic weight of the SWSNN injured randomly is obviously different from that of the uninjured, and the mean of synaptic weight after stabilization decreases gradually with the increase of P.

To show more intuitively the difference in the impact of random attack on the dynamic evolution of synaptic weight of two CSNNs, we further study the relative change rate of the mean of synaptic weight. The relative change rate of the

TABLE 3. The Pearson correlation coefficient between the mean of synaptic weight, and firing rate and membrane potential of SFSNN.

P (%)	5	15	25	35	45
Firing rate	0.974**	0.942**	0.891**	0.856**	0.828**
Membrane potential	-0.915**	-0.935**	-0.892**	-0.843**	-0.882**

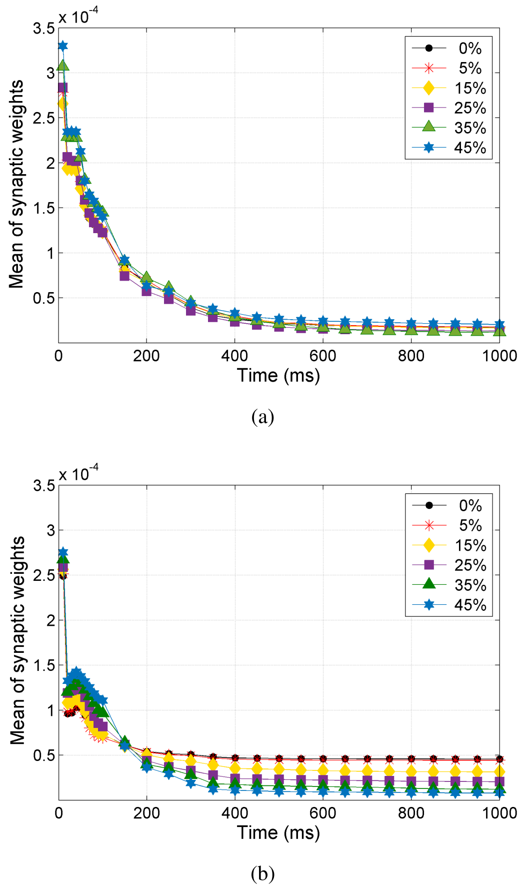

FIGURE 9. The dynamic evolution of the mean of synaptic weight in the CSNNs with different *P*. (a) SFSNN. (b) SWSNN.

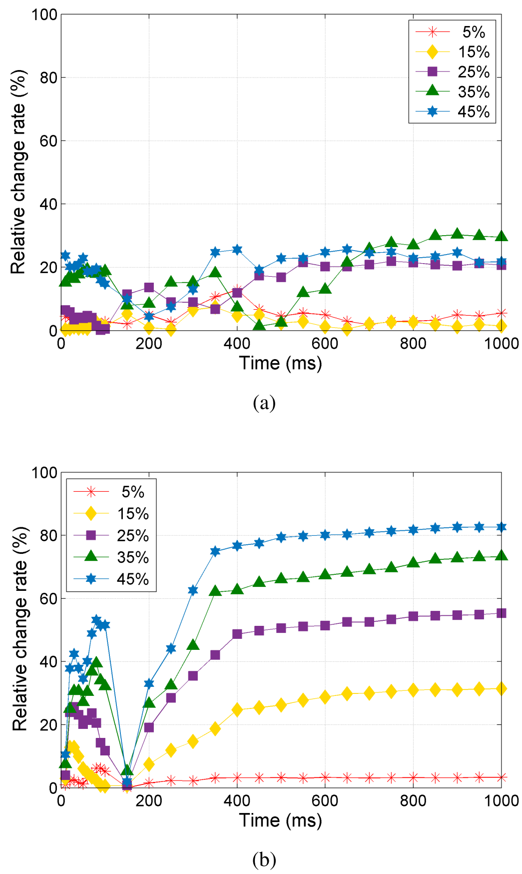

FIGURE 10. The dynamic evolution of the relative change rate of the mean of synaptic weight with time in CSNNs with different *P*. (a) SFSNN. (b) SWSNN.

mean of synaptic weight in CSNNs with different P is shown in Fig. 10.

From Fig. 10(a), for the SFSNN with different P, the evolution processes of the relative change rate of the mean of synaptic weight are slightly different, and the dynamic range of relative change rate is [0%, 30.99%]. From Fig. 10(b), for the SWSNN with different P, the evolution processes of the relative change rate of the mean of synaptic weight are very different, which show an obvious upward trend with the increase of P, and the dynamic range of relative change rate is [0.02%, 82.64%]. Except for the $P = 5\%$, the relative change rate of the mean of synaptic weight after stabilization in SWSNN is higher than that in SFSNN. The results show that the dynamic regulation process of synaptic plasticity of SFSNN is less affected by random attacks than that of SWSNN, which implies the self-adaptive regulation ability of SFSNN is stronger than that of SWSNN under random attacks.

2) CORRELATION ANALYSIS

The Pearson correlation coefficient can reflect the correlation degree between two variables. The t-test can detect the significance of data. In this study, the correlation between the mean of synaptic weight, and firing rate and membrane potential is established based on the Pearson correlation coefficient. The significance level of their correlation is determined by the significance test (two-tailed t-test). If the significance level is 0.05, it is marked with "*"; if the significance level is 0.01, it is marked with "**". The correlation results in SFSNN and SWSNN are shown in Tables 3 and 4, respectively.

From Table 3, for the SFSNN with different P, the mean of synaptic weight is significantly correlated with the firing rate and the membrane potential at 0.01 level. From Table 4, the similar results as SFSNN are obtained in SWSNN. It indicates that the dynamic regulation of synaptic weight is

TABLE 4. The Pearson correlation coefficient between the mean of synaptic weight, and firing rate and membrane potential of SWSNN.

P (%)	5	15	25	35	45
Firing rate	0.892**	0.880**	0.895**	0.878**	0.906**
Membrane potential	-0.992**	-0.993**	-0.990**	-0.987**	-0.992**

significantly correlated with the anti-injury abilities of SWSNN and SFSNN under random attack.

From the above results, the synaptic plasticity of CSNNs with different topologies exhibits different regulation abilities for the same attacks, and the dynamic regulation of synaptic plasticity is significantly related to the anti-injury abilities of CSNNs. It clues that the dynamic regulation of synaptic plasticity is the intrinsic factor of the anti-injury function of CSNNs.

V. CONCLUSION AND FUTURE WORK

In this study, the small-world topology and the scale-free topology are used to construct two kinds of CSNNs with self-adaptive regulation ability, respectively. The anti-injury abilities of two kinds of CSNNs are comparatively analyzed by using the two indexes of the relative change rate of firing rate and the correlation between membrane potential before and after the random attack. On this basis, the information processing of CSNNs under random attacks is analyzed, and the relationship between the dynamic regulation of synaptic plasticity and the anti-injury abilities of the networks is discussed based on the Pearson correlation coefficient. The experimental results demonstrate that: (1) Both CSNNs have a certain anti-injury function, and SFSNN has better performance than SWSNN in the anti-injury ability under random attacks. (2) Under random attacks, the information processing of the anti-injury of CSNN is clarified by the linkage effects of dynamic changes in neuron firing, synaptic weight, and topological characteristics. (3) The dynamic regulation of weight based on synaptic plasticity is significantly correlated with the anti-injury abilities of CSNNs, which implies that the dynamic regulation of synaptic plasticity is the intrinsic factor of the anti-injury function of CSNNs. The findings of this study are helpful to understand brain information processing and promote the development of brain-like intelligence. Moreover, it lays a theoretical foundation for intelligent applications with adaptive fault-tolerance.

The biological brain is composed of many kinds of neurons that perform different brain functions. The SNNs in this study is constructed based on a single-class neuron model, which cannot form multiple brain regions structure and still lacks biological rationality. In our future work, constrained by brain structure and inspired by brain function, we will integrate different kinds of neuron models to construct a SNN with multiple brain regions coordination.

REFERENCES

[1] C. Torres-Huitzil and B. Girau, "Fault and error tolerance in neural networks: A review," *IEEE Access*, vol. 5, pp. 17322–17341, Aug. 2017.

[2] J. Wu, E. Yılmaz, M. Zhang, H. Li, and K. C. Tan, "Deep spiking neural networks for large vocabulary automatic speech recognition," *Frontiers Neurosci.*, vol. 14, Mar. 2020, Art. no. 199.

[3] M. I. Sameen and B. Pradhan, "Landslide detection using residual networks and the fusion of spectral and topographic information," *IEEE Access*, vol. 7, pp. 114363–114373, Aug. 2019.

[4] A. Adineh-vand, G. Karimi, and M. Khazaei, "Digital implementation of a spiking convolutional neural network for tumor detection," *Inf. Midem-J. Microelectron. Electron. Compon. Mater.*, vol. 49, no. 4, pp. 193–201, Dec. 2019.

[5] X. Liu, B. D. Ward, J. R. Binder, S.-J. Li, and A. G. Hudetz, "Scale-free functional connectivity of the brain is maintained in anesthetized healthy participants but not in patients with unresponsive wakefulness syndrome," *PLoS ONE*, vol. 9, no. 3, Mar. 2014, Art. no. e92182.

[6] W. Zheng, H. Yu, W. Ding, L. Guo, G. Xu, and N. Yin, "Changes in brain functional networks of insomniacs induced by magnetic stimulation at acupoints," *IEEE Trans. Appl. Supercond.*, vol. 29, no. 2, pp. 1–4, Mar. 2019.

[7] S. Bin, G. Sun, and C. C. Chen, "Analysis of functional brain network based on electroencephalography and complex network," *Microsyst. Technol.*, early access, Jun. 11, 2019, doi: 10.1007/s00542-019-04424-0.

[8] S.-Y. Kim and W. Lim, "Effect of spike-timing-dependent plasticity on stochastic burst synchronization in a scale-free neuronal network," *Cognit. Neurodyn.*, vol. 12, no. 3, pp. 315–342, Jan. 2018.

[9] B. R. R. Boaretto, R. C. Budzinski, T. L. Prado, J. Kurths, and S. R. Lopes, "Suppression of anomalous synchronization and nonstationary behavior of neural network under small-world topology," *Phys. A, Stat. Mech. Appl.*, vol. 497, no. 1, pp. 126–138, May 2018.

[10] H. Xie, Y. Gong, and B. Wang, "Spike-timing-dependent plasticity optimized coherence resonance and synchronization transitions by autaptic delay in adaptive scale-free neuronal networks," *Chaos, Solitons Fractals*, vol. 108, pp. 1–7, Mar. 2018.

[11] J. Chavas and A. Marty, "Coexistence of excitatory and inhibitory GABA synapses in the cerebellar interneuron network," *J. Neurosci.*, vol. 23, no. 6, pp. 2019–2031, Mar. 2003.

[12] P.-X. Lin, C.-Y. Wang, and Z.-X. Wu, "Two-fold effects of inhibitory neurons on the onset of synchronization in Izhikevich neuronal networks," *Eur. Phys. J. B*, vol. 92, no. 5, May 2019, Art. no. 113.

[13] J. Alstott, M. Breakspear, P. Hagmann, L. Cammoun, and O. Sporns, "Modeling the impact of lesions in the human brain," *PLoS Comput. Biol.*, vol. 5, no. 6, Jun. 2009, Art. no. e1000408.

[14] K. E. Joyce, S. Hayasaka, and P. J. Laurienti, "The human functional brain network demonstrates structural and dynamical resilience to targeted attack," *PLoS Comput. Biol.*, vol. 9, no. 1, Jan. 2013, Art. no. e1002885.

[15] K. W. Thee, H. Nisar, and C. S. Soh, "Graph theoretical analysis of functional brain networks in healthy subjects: Visual oddball paradigm," *IEEE Access*, vol. 6, pp. 64708–64727, Oct. 2018.

[16] R. Albert, H. Jeong, and A.-L. Barabási, "Error and attack tolerance of complex networks," *Nature*, vol. 406, no. 6794, pp. 378–382, Jul. 2000.

[17] S. He, S. Li, and H. Ma, "Effect of edge removal on topological and functional robustness of complex networks," *Phys. A, Stat. Mech. Appl.*, vol. 388, no. 11, pp. 2243–2253, Jun. 2009.

[18] E. M. Izhikevich, "Simple model of spiking neurons," *IEEE Trans. Neural Netw.*, vol. 14, no. 6, pp. 1569–1572, Nov. 2003.

[19] E. M. Izhikevich, J. A. Gally, and G. M. Edelman, "Spike-timing dynamics of neuronal groups," *Cerebral Cortex*, vol. 14, no. 8, pp. 933–944, Aug. 2004.

[20] F. I. Kleberg, T. Fukai, and M. Gilson, "Excitatory and inhibitory STDP jointly tune feedforward neural circuits to selectively propagate correlated spiking activity," *Frontiers Comput. Neurosci.*, vol. 8, p. 53, May 2014.

[21] D. J. Watts and S. H. Strogatz, "Collective dynamics of 'small-world' networks," *Nature*, vol. 393, no. 4, pp. 440–442, Jun. 1998.

[22] D. Wang and X.-Z. Jin, ''On weighted scale-free network model with tunable clustering and congestion,'' *Acta Phys. Sin.*, vol. 61, no. 22, pp. 514–518, Nov. 2012.
[23] V. M. Eguíluz, D. R. Chialvo, G. A. Cecchi, M. Baliki, and A. V. Apkarian, ''Scale-free brain functional networks,'' *Phys. Rev. Lett.*, vol. 94, no. 1, Jan. 2005, Art. no. 018102.
[24] I. E. Antoniou and E. T. Tsompa, ''Statistical analysis of weighted networks,'' *Discrete Dyn. Nature Soc.*, vol. 2008, May 2008, Art. no. 375452.

LEI GUO received the Ph.D. degree in theory and new technology of electrical engineering from the Hebei University of Technology, Tianjin, China, in 2008. He is currently a Ph.D. Supervisor and a Professor with the Hebei University of Technology. His current research interests include neural engineering and brain-like computing.

RUIXUE MAN received the B.S. degree in biomedical engineering from Hebei University, Baoding, China, in 2018. She is currently pursuing the M.S. degree with the Hebei University of Technology. Her current research interest includes neural engineering.

YOUXI WU (Member, IEEE) received the Ph.D. degree in theory and new technology of electrical engineering from the Hebei University of Technology, Tianjin, China, in 2007. He is currently a Ph.D. Supervisor and a Professor with the Hebei University of Technology. His current research interests include data mining and machine learning. He is a Senior Member of CCF.

HUAN LV received the master's degree in biomedical engineering from the Hebei University of Technology, Tianjin, China, in 2019. Her current research interest includes neural engineering.

HONGLI YU received the Ph.D. degree in electrical engineering from the Hebei University of Technology, Tianjin, China, in 2011. She is currently a Ph.D. Supervisor and a Professor with the Hebei University of Technology. Her current research interests include bioelectromagnetic technology and brain science.